Front. Med. 2019, 13(6): 646–657
https://doi.org/10.1007/s11684-018-0643-y

RESEARCH ARTICLE

NES1/KLK10 and *hNIS* gene therapy enhanced iodine-131 internal radiation in PC3 proliferation inhibition

Jiajia Hu[1,*], Wenbin Shen[1,*], Qian Qu[1], Xiaochun Fei[2], Ying Miao[1], Xinyun Huang[1], Jiajun Liu[1], Yingli Wu (✉)[3], Biao Li (✉)[1]

[1]*Department of Nuclear Medicine, Ruijin Hospital Affiliated to Shanghai Jiao Tong University School of Medicine, Shanghai 200025, China;* [2]*Department of Pathology, Ruijin Hospital Affiliated to Shanghai Jiao Tong University School of Medicine, Shanghai 200025, China;* [3]*Hongqiao International Institute of Medicine, Shanghai Tongren Hospital/Faculty of Basic Medicine, Chemical Biology Division of Shanghai Universities E-Institutes, Key Laboratory of Cell Differentiation and Apoptosis of the Chinese Ministry of Education, Shanghai Jiao Tong University School of Medicine, Shanghai 200025, China*

Abstract ***NES1*** **gene is thought to be a tumor-suppressor gene. Our previous study found that overexpression of** ***NES1*** **gene in PC3 cell line could slow down the tumor proliferation rate, associated with a mild decrease in** ***BCL-2*** **expression. The** ***BCL-2*** **decrease could increase the sensitivity of radiotherapy to tumors. Thus, we supposed to have an "enhanced firepower" effect by combining overexpressed** ***NES1*** **gene therapy and ^{131}I radiation therapy uptake by overexpressed hNIS protein. We found a weak endogenous expression of hNIS protein in PC3 cells and demonstrated that the low expression of hNIS protein in PC3 cells might be the reason for the low iodine uptake. By overexpressing** ***hNIS*** **in PC3, the radioactive iodine uptake ability was significantly increased. Results of** ***in vitro*** **and** ***in vivo*** **tumor proliferation experiments and ^{18}F-fluorothymidine (^{18}F-FLT) micro-positron emission tomography/computed tomography (micro-PET/CT) imaging showed that the combined** ***NES1*** **gene therapy and ^{131}I radiation therapy mediated by overexpressed hNIS protein had the best tumor proliferative inhibition effect. Immunohistochemistry showed an obvious decrease of** ***Ki-67*** **expression and the lowest** ***BCL-2*** **expression. These data suggest that via inhibition of** ***BCL-2*** **expression, overexpressed** ***NES1*** **might enhance the effect of radiation therapy of ^{131}I uptake in** ***hNIS*** **overexpressed PC3 cells.**

Keywords androgen-independent prostate cancer; normal epithelial cell-specific 1/kallikrein 10; sodium/iodide symporter; radiation therapy; proliferation

Introduction

Prostate cancer is the most common andropathy in Euro-American countries. The newest statistical cases of this malignant tumor in the USA in 2017 ranked the first place, accounting for 161 360 and makes up 19% in male malignant cases. Moreover, prostate cancer is the third most lethal malignant tumor after lung and rectum cancers [1]. The incidence of prostate cancer in China is lower than in Euro-American countries [2]. However, with the aging and Europeanization of dietary and living habits, the disease incidence is rising every year. In addition, the early diagnosis and treatment are lagging behind in developed countries. As a result, the stage of patients in many areas becomes metaphase or reaches the advanced stages with less opportunity provided for radical cure.

Radical cure includes bath radical prostatectomy and radiotherapy [3,4], which fits the patients with early and limited prostate cancer [5]. The patients with advanced prostate cancer in progressive stage and metastasis are fit for prostatectomy or castrate treatment combined with radiotherapy [6]. During the early stage of the therapy, most of the patients have good curative effect, with clinical manifestations of the regression of tumor and level of prostate-specific antigen (PSA) and the relief of symptoms. However, after 12–33 months of androgen deprivation therapy, the patients are gradually converted to androgen

Received October 10, 2017; accepted April 26, 2018
Correspondence: Yingli Wu, wuyingli@shsmu.edu.cn;
Biao Li, lb10363@rjh.com.cn

*These authors contributed equally to this work.

independence, or even castration-resistant prostate cancer (CRPC) with very unfavorable prognosis [7,8]. Chemotherapy and new endocrine therapy drugs, including docetaxel, enulide, and abitron, can only temporarily prolong the survival time of patients with CRPC (2.8–4.8 months) [9,10]. Thus, the focus of this research is to discover effective therapy for prostate cancer.

Increasing studies have found that the development and progression of prostate cancer are associated with the disturbance of different signaling pathways caused by mutations in a variety of different genes, including the inactivation of important tumor-suppressor genes and the activation of oncogenes [11,12]. The normal epithelial cell specific-1 (*NES1*) gene, also known as *KLK10*, is a member of the kallikrein-related peptidase (KLK) family. *NES1* is a secretive type of serine protease and is wildly expressed in breast and prostate tissues [13]. In our previous research, we have found that *NES1* expression was lost in the androgen-independent prostate cancer cell line PC3. Besides, after the *NES1* gene is overexpressed, apoptosis-related gene *BCL-2* expression is decreased. We found that the apoptosis of the tumor cells increased, and the proliferation was also inhibited [14]. This result confirmed the tumor suppressor role of *NES1*. Protein BCL-2 is an important anti-apoptotic protein, which can inhibit the apoptosis by inhibiting the mitochondrial pathway of apoptosis [15]. The expression of anti-apoptotic protein BCL-2 was increased remarkably in drug-resistant CRPC; this factor may be one of the causes of prostate cancer resistance [16].

Single therapy of tumor often does not prevent the occurrence of treatment resistance. Sodium/iodide symporter (NIS) is the trans-membrane glycoprotein of thyroid cells, which can mediate local aggregation of multiple radionuclides, including ^{125}I and ^{131}I; thus, it has been widely applied to the tumor imaging and radiation therapy of different kinds of tumors besides thyroid diseases [17,18]. Considering that the *BCL-2* downregulation may enhance the effect of radiotherapy [19,20], this study aims to observe the combined effect on prostate cancer by combining *NES1* gene therapy with ^{131}I radiation therapy absorbed by hNIS protein to increase the effect of ^{131}I radiation via the downregulated *BCL-2* expression by *NES1* overexpression.

Materials and methods

Reagents and antibodies

Lentiviral plasmids pLVX-CMV-0-IRES-puro were purchased from Shanghai Boyi Bio-tech Inc. (China). Lentivirus packaging plasmids pVSVG/psPAX2 were also purchased from this company. Puromycin and polyberen were obtained from Sigma-Aldrich, Inc., Merck Company (Germany). $Na^{125}I$ and $Na^{131}I$ reagents were purchased from Shanghai Xinke Pharmaceutical Inc. (China). Cell counting kit 8 (CCK-8) cell proliferation kit was purchased from Kumamoto Dongren Chemical Technology Inc. (Japan). Mouse anti-hNIS monoclonal antibody was purchased from EMD Millipore, Inc., Merck Company (Germany). Rabbit anti-KLK10 and mouse anti-Ki-67 monoclonal antibodies and antirabbit and antimouse horseradish peroxidase (HRP)-labeled secondary antibody were purchased from Sigma-Aldrich, Inc., Merck Company (Germany). HRP-β-actin was purchased from Shanghai Kangchen Bio-tech Inc. (China).

Construction of recombinant lentiviral vectors PC3-NES1-hNIS and PC3-hNIS

Recombinant lentiviral double gene therapy vector pLVX-NES1-IRES-hNIS-puro was designed to transcribe *NES1* after the promoter cytomegalovirus (CMV) and to combine *hNIS* by using an internal ribosomal entry site (IRES). The enzyme restriction sites before and after the gene fragment of NES1-IRES-hNIS were *Xho*I and *Bam*HI, respectively, as confirmed by gene sequencing. Recombinant lentiviral single gene therapy vector pLVX-hNIS-puro was designed to transcribe *hNIS* after the promoter CMV. The enzyme restriction site before and after the *hNIS* gene is *Bam*HI and *Xba*I, respectively, confirmed by gene sequencing.

Construction of PC3-NES1-hNIS and PC3-hNIS stably transfected cell lines

The recombinant plasmid pLVX-NES1-IRES-hNIS-puro and the two packaging plasmids (pVSVG and pCMVΔ 8.91) were co-transfected into HEK293T cells by Lipofectamine 2000™ (Invitrogen™/ThermoFisher Scientific Company, USA). After incubation at 37 °C for 48 h, the cell supernatant, which contained NES1-hNIS-puro of the virus solution, was used to transduce *NES1* and *hNIS* genes into PC3 to obtain the *NES1* and *hNIS* overexpressed stable cell line PC3-NES1-IRES-hNIS-puro. Then, 1 μg/mL of puromycin was added for cell screening, which lasted for 2 weeks. Finally, the stably transfected cell line PC3-NES1-hNIS was established. The stable hNIS-overexpressing cell line, named as PC3-hNIS, was obtained by the same method.

Cell lines

Androgen-independent prostate cancer cell line PC3 (ATCC, CRL-1435) was purchased from Shanghai Institute of Cell Biology, Chinese Academy of Sciences (Shanghai, China). HEK293T cell line was provided by Prof. Yingli Wu. PC3-NES1 and PC3-CON cell lines,

which were stably transfected with NES1 and blank vector, were successfully constructed in the previous study [14] and retained in the laboratory. PC3-NES1-hNIS, PC3-hNIS, PC3-NES1, and PC3-CON cell lines were cultured in RPMI1640 medium (Gibco™/ThermoFisher Scientific Company, USA) supplemented with 10% fetal bovine serum (FBS, Gibco™/ThermoFisher Scientific Company, USA) and 100 units/mL penicillin and 100 μg/mL streptomycin at 37 °C and 5% CO_2. HEK293T cell line was cultured in DMEM with 10% FBS at 37 °C in a 5% CO_2 atmosphere.

Western blot

Cells digested by trypsin were harvested and washed with ice-cold 1× phosphate-bufferred saline (PBS) then were lysed with lysis buffer (62.5 mmol/L Tris–HCl, pH 6.8, 100 mmol/L DTT, 2% SDS, 10% glycerol). Protein extract samples were equally loaded on 10% sodium dodecyl sulfate-polyacrylamide gel, electrophoresed, and transferred to an immobilon-polyvinylidene fluoride membrane (Schleicher & Schuell, Dassel, Germany). After blocking with 5% nonfat milk in PBS, the membranes were incubated with the following primary antibodies respectively at 4 °C overnight: NES1 (1:1000), hNIS (1:1000), followed by the corresponding HRP-conjugated secondary antibodies (1:2000). HRP-linked β-actin (1:5000) was finally incubated at room temperature for an hour and used as loading control. All experiments were repeated thrice with similar results. Bands were detected by chemiluminescence by using a Pierce ECL Western Blotting Substrate (Thermo Scientific Pierce, USA) and recorded by an Image Quant LAS-4000 Luminescent Image Analyzer (GE Healthcare, Piscataway, NJ, USA). Western blot bands were quantified using ImageJ2× (2.1.4.7) software and normalized to normalizator signal (β-actin).

In vitro iodine uptake study

PC3-NES1-hNIS, PC3-hNIS, PC3-NES1, and PC3-CON cells (5×10^4 cells/well) were seeded into 24-well plates, incubated at 37 °C in a 5% CO_2 atmosphere overnight. Each well was washed by sterile, ice-cold 1× PBS twice. Then, 0.5 mL of serum-free RPMI1640 culture solution containing 3.7 kBq of $Na^{125}I$ and 10 μmol/L of NaI was added to each well and incubated at 37 °C in a 5% CO_2 incubator for 5 min, 10 min, 30 min, 1 h, 2 h, 4 h, 10 h, and 26 h. Then, the cells were washed thrice with ice-cold 1× PBS and lysed using 0.5 mL/well of NaOH (1 mol/L) at room temperature. The radioactivity (counts/min, cpm) of the cell lysates was measured by an automatic γ-counter (Shanghai Rihuan Company, Shanghai, China), and the time radioactivity curve was plotted. All experiments were repeated thrice with similar results.

In vitro iodine uptake $NaClO_4$ inhibition study

Sodium perchlorate ($NaClO_4$, 30 μmol/L) was added into cells before adding serum-free RPMI 1640 solution containing $Na^{125}I$. Other procedures were the same as described above. The radioactivity of the cell lysates was measured, and the time radioactivity curve was plotted. All experiments were repeated thrice with similar results.

In vitro iodine efflux study

Four kinds of cells (5×10^4 cells/well) were incubated with 0.5 mL of serum-free RPMI1640 culture solution containing 3.7 kBq of $Na^{125}I$ and 10 μmol/L of NaI at 37 °C in a 5% CO_2 incubator for 1 h, which was the uptake pick according to the result of iodine uptake study. Other procedures were similar to that of iodine uptake study. Then, cells were washed thrice with ice-cold 1× PBS and incubated with 0.5 mL of serum-free RPMI 1640 solution containing 10 μmol/L NaI (without radioactive $Na^{125}I$) at 37 °C in 5% CO_2 incubator for 5, 10, 20, 30, 60, and 120 min. The supernatants were removed into the measuring tube and recorded as supernatants. The cells were lysed using 0.5 mL/well of NaOH (1 mol/L) at room temperature and recorded as intracellular specimens. The radioactivity of supernatants and intracellular specimens were measured, and the time radioactivity curve was plotted as described above. All experiments were repeated thrice with similar results.

CCK-8 cell proliferation assay

CCK-8 cell proliferation assay was performed to detect cell activity difference after ^{131}I radiation therapy *in vitro*. PC3-NES1-hNIS, PC3-hNIS, PC3-NES1, and PC3-CON cells (4×10^5 cells/well) were seeded into 6-well flat plates and incubated overnight. Each well was washed by sterile, ice-cold 1× PBS twice. Then, 1 mL of serum-free RPMI 1640 culture solution containing 3.7 MBq of $Na^{131}I$ and 10 μmol/L of NaI was added to each well and incubated at 37 °C in a 5% CO_2 incubator for 16 h. The same volume of 1× PBS and 10 μmol/L NaI serum-free RPMI1640 culture solution was used as a negative control. Then, each well was washed thrice with sterile, ice-cold 1× PBS. After digestion with trypsin, these four kinds of cells after $Na^{131}I$ treatment were seeded into a 96-well plate (5×10^3 cells/well) and incubated for 4 consecutive days at 37 °C in 5% CO_2 atmosphere. To avoid the influence of $Na^{131}I$, PC3-NES1-hNIS, PC3-hNIS, PC3-NES1, and PC3-CON cells without $Na^{131}I$ treatment were seeded into another 96-well plate (5×10^3 cells/well) as control and incubated at 37 °C in another 5% CO_2 incubator for 4 consecutive days. Cellular proliferation was assessed at the moment of cell attachment at approximately 7 h after cells were plated and

then at 24, 48, 72, and 96 h by using a CCK-8 (Dojindo, Kumamoto, Japan) according to the manufacturer's instructions. After being cocultured for 2 h, the absorbance was detected at a wavelength of 450 nm and adjusted at a wavelength of 690 nm. Each experiment was conducted in triplicate and repeated thrice.

Cell clone formation assay

Cell clone formation assay was also performed to detect cell activity difference after ^{131}I radiation therapy *in vitro*. After 16 h treatment of Na^{131}I (3.7 MBq) at 37 °C in a 5% CO_2 incubator, these four kinds of cells were washed thrice with sterile, ice-cold 1× PBS. After digestion with trypsin, cells were seeded into 6-well plates (1×10^3 cells/well) and cultured with 3 mL fresh complete culture medium. Four kinds of cells treated by 1× PBS as negative control were also seeded into 6-well plates (1×10^3 cells/well) and cultured with 3 mL fresh complete culture medium in another 5% CO_2 incubator at 37 °C to avoid the Na^{131}I influence from the treatment groups. The medium in each well was replaced every 4 days. After 16 days' cell culture, each well was washed thrice with ice-cold 1× PBS, fixed by 4% weight/volume (w/v) paraformaldehyde for 30 min and stained by 1% Crystal Violet Staining Solution (Beyotime Inst Biotech) for 2 h. Each experiment was conducted in triplicate and repeated thrice.

Establishment of xenograft tumors in nude mice

Experiments were performed on male nude mice of 4 weeks old purchased from the Experimental Animal Center, Shanghai Jiao Tong University School of Medicine. All animal experiment protocols were performed in accordance with relevant guidelines and approved by the Animal Care and Use Committee of Shanghai Jiao Tong University School of Medicine (Shanghai, China). Target cells were suspended in sterile, ice-cold 1× PBS, and 5×10^6 cells (0.1 mL) were injected into the subcutaneous part of each flank of nude mice with PC3-NES1 or PC3-CON cell suspension on the left side and PC3-NES1-hNIS or PC3-hNIS cell suspension on the right side. The mouse model groups were as follows: the PC3-NES1 (left) and PC3-NES1-hNIS (right) nude mouse model and PC3-CON (left) and PC3-hNIS (right) nude mice model, each with nine mice. Every 4 days, the vital signs were examined, and the mice weight and the tumor size were recorded, including the long (a) and short (b) diameters of tumor. The volume formula is as follows: volume [mm^3] = $ab^2/2$. When the tumor grew large enough (long diameter was up to 1.5 cm) and the weight of each group decreased, three of the PC3-NES1 (left) and PC3-NES1-hNIS (right) nude mice and PC3-CON (left) and PC3-hNIS (right) nude mice were used for ^{131}I *in vivo* imaging. Three of those mice were used for ^{131}I *in vivo* treatment, and the last three were injected with sterile 1× PBS as negative control treatment.

In vivo ^{131}I single-photon emission computed tomography (SPECT) imaging

To detect the iodide uptake ability of hNIS overexpressed PC3 cells *in vivo*, three of the PC3-NES1 (left) and PC3-NES1-hNIS (right) nude mice and PC3-CON (left) and PC3-hNIS (right) nude mice were injected with 3.7 MBq of Na^{131}I through tail vein for each one. Gasification anesthesia was administered and maintained by volume fraction of 3% isoflurane. Mice were spread in prone position and scanned at 30 min after injection by using pinhole collimator static SPECT imaging (Infinia, GE Company, USA). The image acquisition magnification was 1.45, and the matrix was 128×128. SPECT acquisition collected 10^6 counts per projection, and the scan time was 8–10 min. The images were reconstructed using Xeleris software. Then, the mice were sacrificed by cervical dislocation, and the tumors were taken out. The radioactivity (counts/min, cpm) of the tumor tissue was measured by an automatic γ-counter (Shanghai Rihuan Company, Shanghai, China).

In vivo ^{131}I therapy

At the first 2 weeks of the xenograft tumor formation, *L*-thyroxine at a concentration of 5 mg/L was added to the drinking water to maximize ^{131}I uptake by the tumors and to inhibit the uptake by the thyroid gland. Treatment was started when the tumor-long diameter was up to approximately 1.5 cm and the weight of each group decreased. One group (three for each group) of PC3-NES1 (left) and PC3-NES1-hNIS (right) and one group of PC3-CON (left) and PC3-hNIS (right) nude mice were injected with Na^{131}I intraperitoneally twice on days 1 and 14 with 37 MBq (0.2 mL) for each one and each time. The last groups (three for each group) were injected with 0.5 mL sterile 1× PBS in the same manner as negative control treatment. The vital signs of nude mice were observed every 2 days. The mice weight and the tumor size, with long and short diameter, were measured every 7 days after first ^{131}I injection until day 28 by using calipers. At day 29, ^{18}F-fluorothymidine (^{18}F-FLT) micro-positron emission tomography/computed tomography (micro-PET/CT) imaging was performed. The tumor growth curve was drawn with the tumor volume. The tumor inhibition rate (TIR) was calculated as follows: TIR = (Vc – Vt) / Vc×100%, where Vc is the mean volume of transplanted tumors in each control group and Vt is the mean volume of transplanted tumors in each ^{131}I treatment group. All nude mice were sacrificed after ^{18}F-FLT micro-PET/CT imaging. The transplanted tumor

was obtained to compare the size and to undergo immunohistochemical analysis.

^{18}F-FLT micro-PET/CT imaging

All mice treated by ^{131}I therapy and sterile 1× PBS underwent ^{18}F-FLT micro-PET/CT imaging on the Siemens Inveon Micro PET/CT (Inveon MM Platform, Siemens Preclinical Solutions, Knoxville, Tennessee, USA) with a computer-controlled bed and 8.5 cm transaxial and 5.7 cm axial fields of view. The imaging method was based on previous studies [14]. Mice were anesthetized with 3% volume/volume (v/v) isoflurane in O_2 gas for ^{18}F-FLT tail intravenous injection (a single injection of 0.2 mL at an activity of 5.3–6.4 MBq). Waiting for 30 min post injection, mice were first computed tomography (CT) scanned for 20 min and then continuously positron emission tomography (PET) scanned for 5 min. Mice were anesthetized with 1.5% v/v isoflurane during scanning. Inveon Acquisition Workplace (IAW) was used for scanning. The CT data were used for both scatter and attenuation correction. Images were reconstructed by an OSEM3D (Three-Dimensional Ordered Subsets Expectation Maximum) algorithm followed by Maximization/Maximum a Posteriori (MAP) or Fast MAP provided by IAW. The 3D regions of interest were drawn over the tumor tissue guided by CT images, and tracer uptake was measured using the software of Inveon Research Workplace 3.0. Individual quantification of the ^{18}F-FLT uptake in each of them was calculated to obtain the SUVmax.

Immunohistochemistry

After the ^{18}F-FLT micro PET/CT imaging of each group, the mice were sacrificed by cervical dislocation, and the tumors were harvested. Then, the tumor tissue was bar cut into almost 1 mm^3, immobilized in 4% w/v paraformaldehyde, embedded, and chipped. Tumor tissue sections were prepared into a 4 μm section from paraffin-embedded block and then subjected to immunohistochemical analysis by using mouse anti-hNIS antibody (1:200), rabbit anti-KLK10 antibody (1:200), and mouse anti-Ki-67 antibody (1:200). The experimental method was based on previous studies [14].

Statistical analysis

Statistical analysis was performed using GraphPad Prism 5.0 software. The comparison of mean of each group was analyzed by one-way ANOVA. Statistical comparisons between the two groups were performed using Student's *t* tests. A value of $P < 0.05$ (*) was considered statistically significant, $P < 0.01$(**) and $P < 0.001$(***) were considered remarkably significant, and $P > 0.05$ (ns) was considered no difference. Data were presented as the mean with standard deviation (SD) in the line or bar graphs.

Results

Expression of NES1 and hNIS protein in four kinds of PC3 cell lines and verification of function of overexpressed hNIS protein in PC3 cell lines by radioactive iodine uptake-related studies *in vitro* and *in vivo*

The results of Western blot (Fig. 1A) showed that the expression of NES1 and hNIS protein in PC3-NES1-hNIS cell line and hNIS protein in PC3-hNIS cell line were obvious in accordance with the expectation. Interestingly, weak expression of hNIS protein in PC3-NES1 and PC3-CON cell lines were also detected. This finding suggested the endogenous expression of hNIS protein in PC3 cell line. However, less iodine uptake capacity could be detected in PC3-CON and PC3-NES1 cell lines by *in vitro* ^{125}I uptake-related studies (Fig. 1B). The function of overexpressed hNIS protein in PC3-NES1-hNIS and PC3-hNIS cell lines was obvious. In ^{125}I uptake study, the peak of iodine uptake in PC3-NES1-hNIS cell line occurred at 2 h with a slow rise stage between 30 min and 2 h, and the peak value was 4.6-fold higher than that of PC3-NES1 and PC3-CON cell lines at the same time point. After 2 h, the uptake value decreased gradually and slowly. However, the iodine capacity was still three-fold higher than that of control cell lines at 26 h. In PC3-hNIS cell line, because of the liaison of *hNIS* gene directly behind of CMV promoter, the peak value of iodine uptake was higher than that of PC3-NES1-hNIS cell line, with 6.2-fold higher than that of control cell lines. However, the peak time of PC3-hNIS cell line occurred early at 1 h without obvious slow rise stage. After 1 h, the uptake value decreased gradually, and the iodine capacity was 3.1-fold higher than that of control cell lines at 26 h (Fig. 1B). The iodine uptake capacity of both cell lines could be completely inhibited by 30 μmol/L $NaClO_4$ (Fig. 1C). Given that the internalized iodide cannot be organified as the organic iodide polymer and neither can it be stored in PC3-NES1-hNIS and PC3-hNIS cells like in thyroid cells, Na^{125}I was rapidly effluxed from both cell lines, maintaining for approximately 1 h (Fig. 1D).

Animal SPECT imaging further confirmed the iodine uptake ability of hNIS protein *in vivo* (Fig. 1E–1H). After 30 min of Na^{131}I injection (3.7 MBq/mouse) in the tail vein of the nude mice, SPECT imaging showed the radioactive iodine uptake of subcutaneous PC3-NES1-hNIS and PC3-hNIS xenografts (red and yellow circles), which were significantly higher than PC3-NES1 and PC3-CON xenografts, respectively (green and purple circles). Significant radioiodine accumulation was also observed in

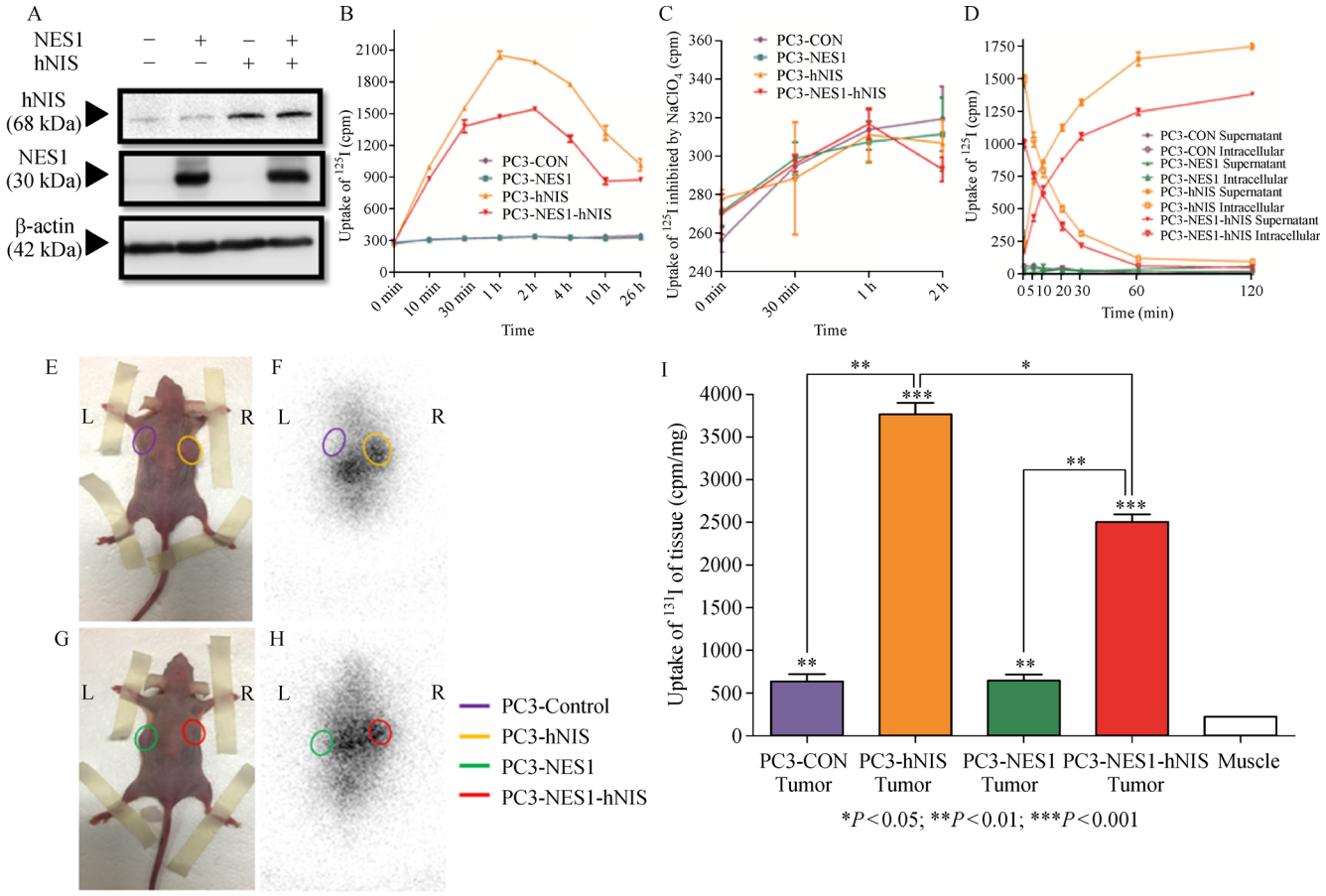

Fig. 1 Expression of NES1 and hNIS protein in four kinds of PC3 cell lines and verification of function of overexpressed hNIS protein in PC3 cell lines by radioactive iodine uptake related studies *in vitro* and *in vivo*. (A) Western blot confirmed the obvious expression of NES1 and hNIS protein in PC3-NES1-hNIS cell line and hNIS protein in PC3-hNIS cell line. Interestingly, weak expression of hNIS protein in PC3-NES1 and PC3-CON cell lines were also detected. (B) The function of overexpressed hNIS protein in PC3-NES1-hNIS and PC3-hNIS cell lines was verified by ^{125}I uptake study. Less iodine uptake capacity could be detected in PC3-CON and PC3-NES1 cell lines. (C) *In vitro* iodine uptake $NaClO_4$ inhibition study showed that the iodine uptake capacity of PC3-NES1-hNIS and PC3-hNIS cell lines could be completely inhibited by 30 μmol/L $NaClO_4$. (D) *In vitro* iodine efflux study showed that $Na^{125}I$ was rapidly effluxed from both PC3-NES1-hNIS and PC3-hNIS cell lines, maintaining for approximately 1 h. (E–H) Animal SPECT imaging further confirmed the iodine uptake ability of hNIS protein *in vivo*. This observation showed that the radioactive iodine uptake of subcutaneous PC3-NES1-hNIS and PC3-hNIS xenografts (red circle and yellow circle) was significantly higher than that of PC3-NES1 and PC3-CON xenografts, respectively (green circle and purple circle). Radioiodine accumulation in PC3-NES1 and PC3-CON xenografts was almost invisible. (I) Quantitative analysis by the automatic γ-counter demonstrated a significantly high radioactivity in PC3-hNIS and PC3-NES1-hNIS xenograft tissue compared with that in muscle tissue (17.8-fold and 11.8-fold, $P < 0.001$), a low radioactivity in PC3-NES1, and PC3-CON xenograft tissue compared with that in muscle tissue (3.0-fold respectively, $P < 0.01$). The iodine uptake capacity of PC3-hNIS and PC3-NES1-hNIS xenograft was much higher than that of PC3-CON and PC3-NES1 xenograft ($P < 0.01$), and the uptake capacity of PC3-hNIS was 1.5-fold higher than that of PC3-NES1-hNIS ($P < 0.05$).

tissues which expressed endogenous NIS, including the thyroid and stomach. Although PC3-NES1 and PC3-CON cell lines expressed slightly endogenous NIS protein, radioiodine accumulation in these two xenografts was almost invisible. To avoid the uptake influence from other organs, we removed the xenografts to detect the radioactivity (Fig. 1I). Quantitative analysis by the automatic γ-counter demonstrated a significantly high radioactivity in PC3-hNIS and PC3-NES1-hNIS xenograft tissues (17.8-fold and 11.8-fold, $P < 0.001$), a low radioactivity in PC3-NES1, and PC3-CON xenograft tissue (3.0-fold respectively, $P < 0.01$) compared with the muscle tissue. The iodine uptake capacity of PC3-hNIS xenograft was 1.5-fold higher than that of PC3-NES1-hNIS ($P < 0.05$). This finding was consistent with the radioiodine uptake study result *in vitro*.

Cell proliferation was reduced significantly by combined treatment of *NES1* and ^{131}I

Four groups of PC3 cell lines (4×10^5 cells/well) were treated with ^{131}I (3.7 Mq/well) for 16 h, and as control, other four groups were treated with equal volume of 1× PBS at the same time. Then, those eight group cell lines were performed CCK-8 cell proliferation assay for 4 consecutive days. The result showed an obvious inhibitive effect in the single *NES1* gene therapy group PC3-NES1, single ^{131}I treatment absorbed by the hNIS protein group PC3-hNIS with ^{131}I, and the combined treatment group PC3-NES1-hNIS cell line with ^{131}I (Fig. 2A). As we expected, the combined treatment group grew the slowest. The combined treatment group grew significantly slower than the single *NES1* gene treatment group PC3-NES1 cell line ($P < 0.001$) and was significantly slower than the PC3-hNIS cell line treated with ^{131}I ($P < 0.001$). The single *NES1* gene therapy group PC3-NES1 and the single ^{131}I treatment group PC3-hNIS cell line with ^{131}I also had an inhibitive effect compared with the control group ($P < 0.001$ and $P < 0.01$, respectively). However, these cell lines were still growing in the first few days after ^{131}I treatment. The inhibitive effect was much more intuitive and significant in cell clone formation assay, which lasted for 16 days. This result showed the most significant inhibition proliferative effect in PC3-NES1-hNIS cells treated with ^{131}I (Fig. 2B). Slow proliferation was also found in the PC3-NES1 group and the PC3-hNIS group with single ^{131}I treatment. The finding was consistent with the result of CCK-8 cell proliferation assay. Quantitative analysis by Image-Pro Plus software showed the same result (Fig. 2C). Compared with the PC3-CON group, the combined treatment group grew significantly the slowest ($P < 0.001$). A significant inhibitive effect was also observed in the PC3-NES1 group ($P < 0.001$) and the PC3-hNIS group treated with ^{131}I ($P < 0.01$). Compared with the PC3-NES1 group and the PC3-hNIS group treated with ^{131}I, the combined treatment group grew significantly the slowest ($P < 0.001$).

Best therapeutic effect of combined treatment of *NES1* and ^{131}I in PC3 xenograft tumors expressing NES1 and hNIS *in vivo*

Tumor volume line graph showed a proliferative inhibition effect on PC3-NES1 and PC3-NES1-hNIS xenograft from the beginning (Fig. 2D). The effect was significant since day 24 compared with the PC3-CON and PC3-hNIS groups ($P < 0.05$). The weight change of each group of nude mice had no obvious significance, whereas the groups loaded with PC3-NES1 and PC3-hNIS-NES1 xenografts increased slightly faster than those loaded with PC3-CON and PC3-hNIS (Fig. 2E). After day 24, the weight of each group declined. At day 32, when the tumor long diameter was up to approximately 1.5 cm, we started the radioactive iodine-131 treatment, with an injection of 37 MBq per mouse. Without a significant inhibitive effect, at day 46, we performed the second radioactive iodine-131 treatment with the same radioactivity. After two times radiation treatment, the tumor volume of PC3-hNIS-NES1 and PC3-hNIS with the ^{131}I groups grew slowly and started to decline. An obvious therapeutic effect could be found in PC3-hNIS-NES1 with the ^{131}I groups ($P < 0.01$). The growth of PC3-NES1 xenograft was always slower than that of the PC3-CON group ($P < 0.05$). The growth of PC3-hNIS xenograft with ^{131}I treated was also slower than that of the PC3-CON group, but the difference was not significant (Fig. 2D and 2F). After ^{131}I treatment, the weight of PC3-hNIS-NES1 in the ^{131}I group declined the slowest ($P < 0.01$, Fig. 2E). This result showed that combined therapy did not affect food intake or physical activity. By comparing the tumor volume difference between treatment and the control groups, TIR (mean % ± SD%) was as follows: 83.54% ± 8.79%, 51.91% ± 6.90%, and 32.46% ± 17.97% for PC3-hNIS-NES1 with ^{131}I and PC3-NES1 and PC3-hNIS with ^{131}I, respectively (Fig. 3G). Compared with single *NES1* gene therapy and single radioactive iodine-131 treatment, combined treatment had the best TIR ($P < 0.01$ and $P < 0.05$, respectively).

Combined treatment of *NES1* and ^{131}I in PC3 xenograft tumors inhibited the tumor proliferation associated with the downregulation of BCL-2 expression

Before sacrificing the nude mice, we performed ^{18}F-FLT micro-PET/CT imaging to evaluate the tumor proliferation *in vivo* (Fig. 3A). The combined therapy group (PC3-hNIS-NES1 with ^{131}I) decreased the volume of xenograft and the ^{18}F-FLT uptake. The volume of PC3-CON xenograft with and without ^{131}I treatment was large. The uptake was also high (Fig. 3B). Bar chart of ^{18}F-FLT uptake in xenograft showed that the SUV_{max} of PC3-NES1-hNIS xenograft tumors with ^{131}I treatment was the lowest in these eight groups. Compared with the PC3-CON group and two single treatment groups, the difference was significant ($P < 0.01$, $P < 0.05$, and $P < 0.05$, respectively). Single radioactive iodine-131 treatment could also decrease the SUV_{max} of ^{18}F-FLT uptake in xenograft tissue ($P < 0.05$). Single *NES1* gene therapy could decrease the ^{18}F-FLT uptake, whereas the difference was not so significant (Fig. 3B). Immunohistochemistry showed an obvious decrease of *Ki-67* expression in two single-treated groups and PC3-NES1-hNIS with the ^{131}I group. The latter had the lowest expression (Fig. 3C). This result was consistent with all other results of experiments *in vivo*. Based on the previous study [14], we detected that the *BCL-2* expression in xenograft tissue with combined therapy was the lowest. In addition, both single *NES1*

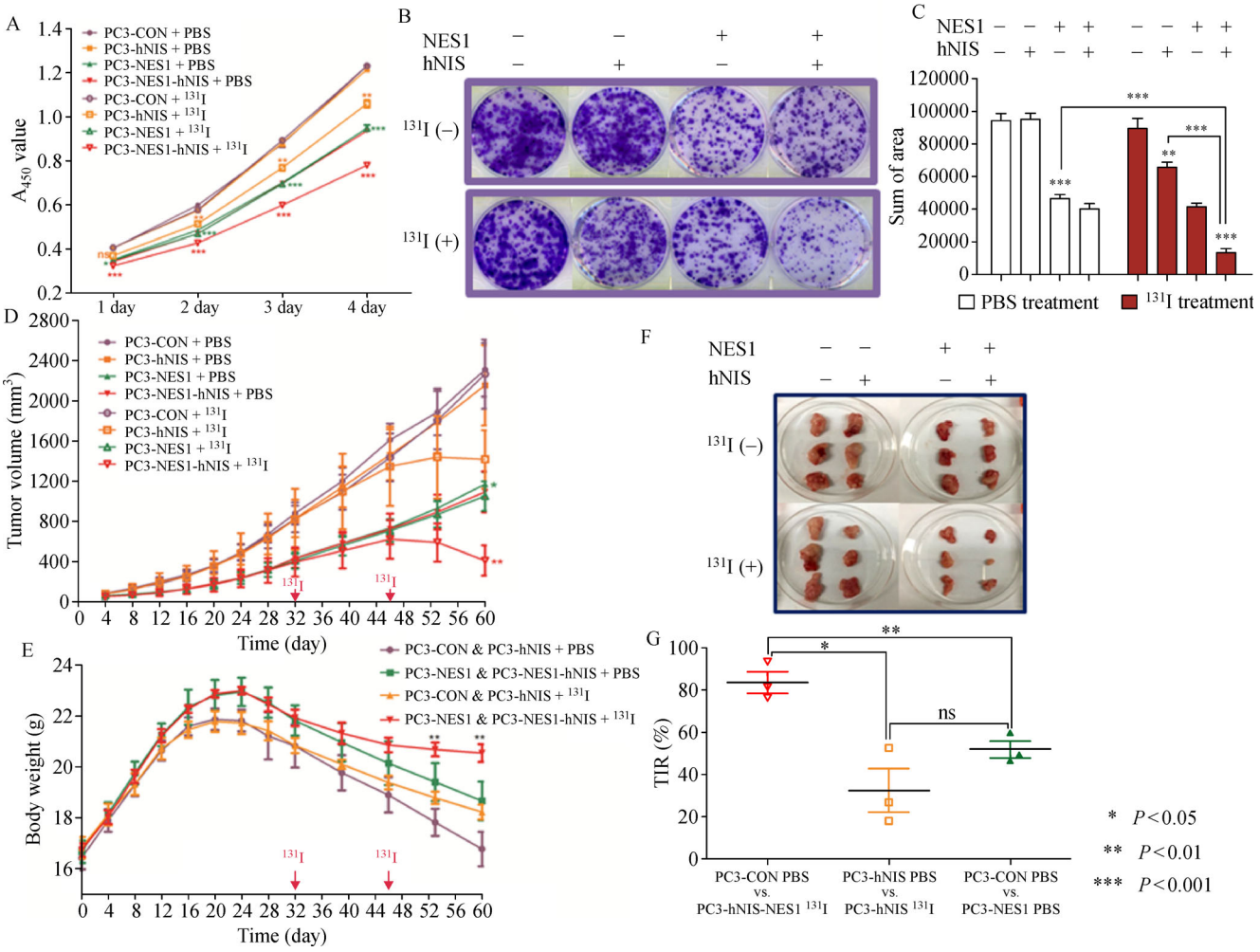

Fig. 2 Best therapeutic effect of the combined treatment of *NES1* and ^{131}I on PC3 cell lines and xenograft tumors. (A) CCK-8 cell proliferation assay showed an obvious inhibitive effect in the single *NES1* gene therapy group PC3-NES1 ($P < 0.001$), single ^{131}I treatment absorbed by the hNIS protein group PC3-hNIS with ^{131}I ($P < 0.01$), and the combined treatment group PC3-NES1-hNIS cell line with ^{131}I ($P < 0.001$). The combined treatment group grew significantly slower than the single *NES1* gene treatment group PC3-NES1 cell line ($P < 0.001$) and significantly slower than the PC3-hNIS cell line treated with ^{131}I ($P < 0.001$). (B) Cell clone formation assay, which lasted for 16 days, showed the most significant proliferative inhibition in PC3-NES1-hNIS cells treated with ^{131}I. A significant inhibition effect was also found in the PC3-NES1 group and the PC3-hNIS group with single ^{131}I treatment. The finding was consistent with the result of CCK-8 cell proliferation assay. (C) Quantitative analysis of cell clone formation assay by Image-Pro Plus software showed the same result. Compared with the PC3-CON group, the combined treatment group significantly grew the slowest ($P < 0.001$). A significant inhibitive effect was also observed in the PC3-NES1 group ($P < 0.001$) and the PC3-hNIS group treated with ^{131}I ($P < 0.01$). Compared with the PC3-NES1 group and the PC3-hNIS group treated with ^{131}I, the combined treatment group grew significantly the slowest ($P < 0.001$). (D) Tumor volume line graph showed a proliferative inhibition effect on PC3-NES1 and PC3-NES1-hNIS xenograft from the beginning. At days 32 and 46, ^{131}I systematic therapy was performed twice, with an injection of 37 MBq each. An obvious therapeutic effect could be found in PC3-hNIS-NES1 with the ^{131}I groups ($P < 0.01$). The growth of PC3-NES1 xenograft was always slower than that of the PC3-CON group ($P < 0.05$). The growth of PC3-hNIS xenograft with ^{131}I treatment was also slower than that of the PC3-CON group, but the difference was not significant enough. (E) Nude mice body weight line graph showed that the body weight change of each group of nude mice had no obvious significance. However, those loaded with PC3-NES1 and PC3-hNIS-NES1 xenografts increased slightly faster than those loaded with PC3-CON and PC3-hNIS. After day 24, the weight of each group decreased. After ^{131}I treatment, the weight of PC3-hNIS-NES1 with ^{131}I group declined the slowest ($P < 0.01$). (F) General images showed that the tumor volume of PC3-hNIS-NES1 with the ^{131}I groups was the smallest. Single *NES1* gene therapy and single ^{131}I of radiation therapy mediated by the hNIS protein overexpressed groups also had an inhibitive effect compared with the control groups. (G) Tumor inhibition rate (TIR) (mean% ± SD%) was as follows: 83.54% ± 8.79%, 51.91% ± 6.90%, and 32.46% ± 17.97% for PC3-CON with PBS vs. PC3-hNIS-NES1 with ^{131}I, PC3-CON with PBS vs. PC3-NES1 with PBS, PC3-hNIS with PBS vs. PC3-hNIS with ^{131}I, respectively. Compared with single *NES1* gene therapy and single radioactive iodine-131 treatment, combined treatment had the best tumor inhibition rate ($P < 0.01$ and $P < 0.05$, respectively).

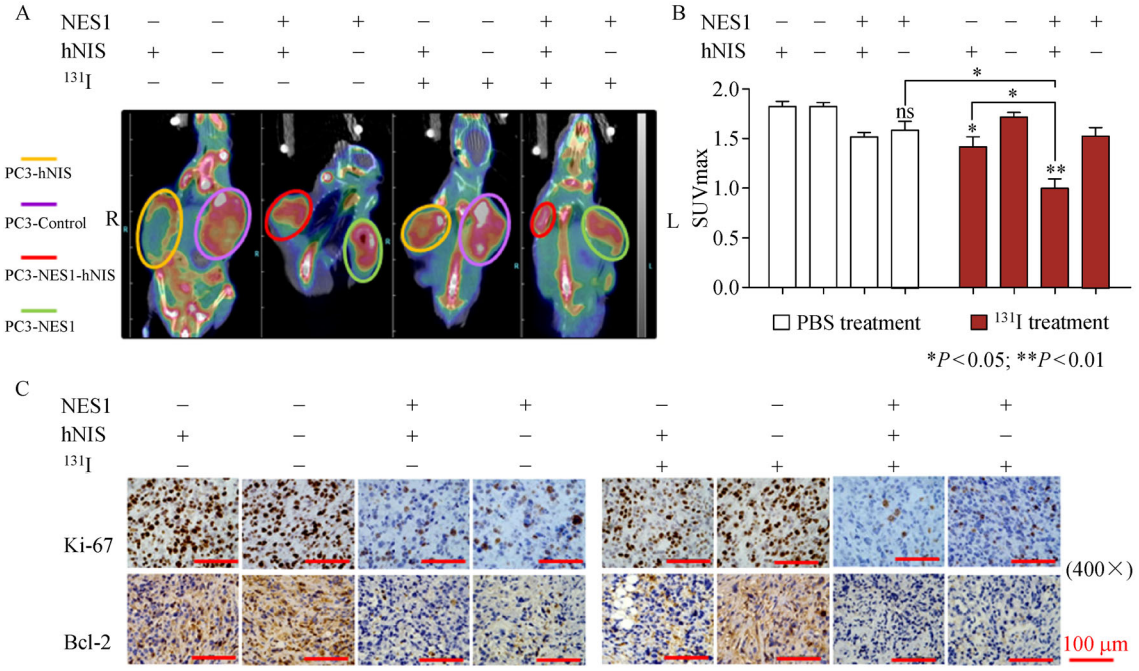

Fig. 3 Combined therapy of *NES1* and ^{131}I in PC3 xenograft inhibited the tumor proliferation associated with downregulation of *BCL-2* expression. (A)^{18}F-FLT micro-PET/CT imaging, which could evaluate the tumor proliferation *in vivo*, showed that the combined therapy group (PC3-hNIS-NES1 with ^{131}I) obviously decreased the volume of xenograft and the ^{18}F-FLT uptake. The volume of PC3-CON xenograft with and without ^{131}I treatment was large. The uptake was also high. (B) Bar chart of ^{18}F-FLT uptake in xenograft showed that the SUV_{max} of PC3-NES1-hNIS xenograft tumors with ^{131}I treatment was the lowest in these eight groups. Compared with the PC3-CON group and two single treatment groups, the difference was significant ($P < 0.01$, $P < 0.05$, and $P < 0.05$, respectively). Single radioactive iodine-131 treatment could also decrease the SUV_{max} of ^{18}F-FLT uptake in xenograft tissue ($P < 0.05$). Single *NES1* gene therapy could decrease the ^{18}F-FLT uptake, but the difference was not so significant. (C) Immunohistochemistry showed an obvious decrease of *Ki-67* expression in two single-treated groups and PC3-NES1-hNIS with the ^{131}I group. The latter showed the lowest expression. In addition, the *BCL-2* expression in the xenograft tissue of both single-treated groups and PC3-NES1-hNIS with the ^{131}I group decreased obviously. The latter was the lowest.

gene therapy and single radioactive iodine-131 treatment could decrease the *BCL-2* expression (Fig. 3C).

Discussion

NES1 gene is thought to be a tumor-suppressor gene, which decreased the expression in prostate cancer tissues but is expressed in the normal prostate tissues [21]. The lack of *NES1* expression is due to the hypermethylation of its exon 3 CpG island [22]. The anticancer effect was first discovered in related studies about *NES1* gene therapy of breast cancer, showing that overexpression of *NES1* gene or demethylation of its exon3 CpG island could inhibit tumor proliferation [21]. Our previous study [14] and this study found that overexpression of *NES1* gene in PC3 cell line could slow down the proliferation rate of PC3 cells and its xenograft tumor. However, the tumor volume was still increasing. These results indicated that the desired effect of tumor inhibition was not easy to be achieved by single gene therapy. Similar to many current cancer treatment programs, single gene therapy is no longer able to be the only treatment regimen. Thus, to combine chemotherapy or radiotherapy on the basis of gene therapy to obtain a possible radical cure is necessary [23].

Prostate cancer is one of the most popular types of neoplasms treated by radioactive iodine therapy mediated by *hNIS* gene. From the earliest works about *hNIS* gene transported by simple adenovirus vector into tumor cell to mediate ^{131}I therapy *in vivo* [24] to late ones utilizing tumor-targeted oncolytic virus as vector [17,25], the tumor inhibition effect of this method has been confirmed by many preclinical studies. Moreover, some researchers have conducted phase I clinical trials to confirm the feasibility of this "radiovirus treatment" [18]. The results showed that tumor cells could be killed in patients with localized prostate cancer. The advantage of *hNIS* gene is that it could not only be used for the report gene imaging to monitor the expression reliability of targeted gene and diagnostic

localization of tumor but also be used for the radionuclide therapy by ^{131}I uptake. This phenomenon suggested that by inducing the expression of hNIS protein uptaking ^{131}I in prostate cancer, ^{131}I internal radiation therapy would be beneficial to patients, especially those with systemic metastasis of prostate cancer. Given that this treatment does not depend on the dependence of the tumor on androgen, this therapy might be an effective treatment for patients with CRPC.

However, single radiation therapy is also not enough for prostate cancer treatment. This study showed that ^{131}I treatment could slow down the tumor growth, but the effect was not good enough. The TIR was only 32.46% ± 17.97%. Our previous study found that *NES1* overexpression was associated with a mild decrease in *BCL-2* expression in PC3 cells [14]. According to some literatures, the decrease in *BCL-2* expression could increase the sensitivity of radiotherapy to tumors [19,20]. We supposed to have an "enhanced firepower" effect by combining *NES1* gene therapy and ^{131}I radiation therapy uptake by hNIS protein. Thus, we performed those related functional experiments to evaluate the combined therapy effect on prostate cancer proliferation by using PC3-NES1-hNIS stably transfected cell line.

In this study, we co-expressed *NES1* and *hNIS* genes in PC3 cell line and confirmed the expression by Western blot. Interestingly, we found light endogenous expression of hNIS protein in PC3-NES1 and PC3-CON cell lines. However, this endogenous protein had much less radioactive iodine uptake function in those cells than *hNIS*-overexpressed cell lines PC3-NES1-hNIS and PC3-hNIS. The animal SPECT imaging also confirmed the function of *hNIS*-overexpressed cell lines PC3-NES1-hNIS and PC3-hNIS xenograft *in vivo*, thereby showing that radioactive iodine uptake imaging in xenograft tissues of PC3-NES1 and PC3-CON was not obvious. We wondered whether the endogenous hNIS protein in PC3 cell line lost its iodine uptake function. Quantitative analysis by the automatic γ-counter demonstrated a low radioactive iodine uptake in PC3-NES1 and PC3-CON xenograft tissues, i.e., 3.0-fold of that of muscle tissue. Low expression of hNIS protein in PC3 cell line might have led to low iodine uptake. Overexpression of hNIS protein in PC3 cell line could enhance the iodine uptake in PC3 cell line.

Through *in vitro* and *in vivo* tumor proliferation studies and the ^{18}F-FLT Micro-PET/CT imaging, combining *NES1* gene therapy with ^{131}I radiation therapy uptake by hNIS protein overexpressed had a best tumor proliferative inhibition effect. This therapy could decrease the growth line of tumor rather than simply slowing down the growth rate. Immunohistochemistry showed a significant decrease of *Ki-67* expression in PC3-NES1-hNIS xenograft tumor treated with ^{131}I. This finding confirmed the results of those functional experiments. In addition, the weight of this group declined the slowest. This result showed that combined therapy did not affect food intake or physical activity and even gave a good life quality.

In this study, immunohistochemistry showed that both single *NES1* gene therapy and single radioactive iodine-131 treatment could decrease the *BCL-2* expression. This method could be the reason for tumor proliferation inhibition. Zhao *et al.* confirmed the role of ^{131}I in cell proliferation in a thyroid cancer cell line by inhibition of *BCL-2* expression in a dose-dependent manner and by upregulation of B cell translocation gene 2-mediated activation of JNK/NF-κB pathways [26]. In addition, the *BCL-2* expression in xenograft tissue with combined therapy was the lowest. The treatment effect was also the best. This finding suggested that overexpressed NES1 via inhibition of the *BCL-2* expression could enhance the effect of ^{131}I radiation. The exact underlying mechanism of *BCL-2* downregulation is unknown. In our previous study [14], *NES1/KLK10* upregulation decreases *BCL-2* expression and Hexokinase2 (*HK2)* in PC3 cells. Moreover, *HK2* downregulation could reduce BCL-2 protein. Thus, *KLK10* could decrease *BCL-2* through *HK2* downregulation. Further molecular mechanism should be explored in future experiments.

Gene therapy for prostate cancer has been used for clinical trials [23] for those patients with locally recurrent prostate cancer or progressive diseases, such as CRPC. However, manipulation of two target genes still has its limitations, including targeting and expression, especially in relation to the transport vector. In our study, we used lentiviral plasmids pLVX-CMV-0-IRES-puro as vector and used IRES to separate *NES1* and *hNIS* gene to express them, respectively, and to avoid the formation of fusion protein. The protein expression and function results were promising. The targeting will be solved in the future.

In summary, although this study was similar to the pattern of basic studies about gene therapy combined with internal radiation therapy, this work was the first time to combine *NES1* and *hNIS* gene therapy with ^{131}I internal radiation therapy mediated by *hNIS* overexpressed for androgen-independent prostate cancer. The combined treatment had efficacy, and a promising result was achieved. PC3 cells had a weak *hNIS* expression, and overexpression of hNIS protein in PC3 cell line could enhance the cell iodine uptake. *BCL-2* downregulation might be the key point of the good combined effect. Further molecular mechanism should be explored in future experiments. Besides, to perform transformation studies or even clinical trials carried out for systematic treatment, a suitable transport vector is needed, such as a safe-targeted virus or a safe nanocarrier. Furthermore, regarding the dose of ^{131}I systematic therapy, the present study found a significant therapeutic effect in the short-term (4 weeks) after treatment with the therapeutic schedule of twice injection of 37 MBq each at an interval of 2 weeks. The next step is to study whether a combination therapy

involving a small dose of ^{131}I also has the same antitumor effect and the time of onset. These results could be an experimental basis for future clinical application.

Acknowledgements

This study was financially supported by the foundation from the National Natural Science Foundation of China (Nos. 81501502 and 81570118), Scientific Research Project of Shanghai Municipal Commission of Health and Family Planning (No. 201740154), Multidisciplinary Cross-Project (Medical) of Shanghai Jiao Tong University (No. YG2017MS65), and the foundation of talent plan A for Guangci Excellent Youth of Ruijin Hospital Affiliated to Shanghai Jiao Tong University School of Medicine (No. GCQN-2017-A12), and the National Key R&D Program of China (No. 2017YFA 0505200).

Compliance with ethics guidelines

Jiajia Hu, Wenbin Shen, Qian Qu, Xiaochun Fei, Ying Miao, Xinyun Huang, Jiajun Liu, Yingli Wu, and Biao Li declare no conflicts of interests. All institutional and national guidelines for the care and use of laboratory animals were followed.

References

1. Siegel RLMK, Jemal A. Cancer Statistics, 2017. CA Cancer DJ Clin 2017; 67: 23
2. Chen R, Sjoberg DD, Huang Y, Xie L, Zhou L, He D, Vickers AJ, Sun Y; Chinese Prostate Cancer Consortium; Prostate Biopsy Collaborative Group. Prostate specific antigen and prostate cancer in Chinese men undergoing initial prostate biopsies compared with western cohorts. J Urol 2017; 197(1): 90–96
3. Mohler JL, Kantoff PW, Armstrong AJ, Bahnson RR, Cohen M, D'Amico AV, Eastham JA, Enke CA, Farrington TA, Higano CS, Horwitz EM, Kane CJ, Kawachi MH, Kuettel M, Kuzel TM, Lee RJ, Malcolm AW, Miller D, Plimack ER, Pow-Sang JM, Raben D, Richey S, Roach M 3rd, Rohren E, Rosenfeld S, Schaeffer E, Small EJ, Sonpavde G, Srinivas S, Stein C, Strope SA, Tward J, Shead DA, Ho M; National Comprehensive Cancer Network. Prostate cancer, version 2.2014. J Natl Compr Canc Netw 2014; 12(5): 686–718
4. Heidenreich A, Aus G, Bolla M, Joniau S, Matveev VB, Schmid HP, Zattoni F; European Association of Urology. EAU guidelines on prostate cancer. Eur Urol 2008; 53(1): 68–80
5. Williams SB, Huo J, Chamie K, Smaldone MC, Kosarek CD, Fang JE, Ynalvez LA, Kim SP, Hoffman KE, Giordano SH, Chapin BF. Discerning the survival advantage among patients with prostate cancer who undergo radical prostatectomy or radiotherapy: the limitations of cancer registry data. Cancer 2017; 123(9): 1617–1624
6. Pagliarulo V, Bracarda S, Eisenberger MA, Mottet N, Schröder FH, Sternberg CN, Studer UE. Contemporary role of androgen deprivation therapy for prostate cancer. Eur Urol 2012; 61(1): 11–25
7. Bolla M, de Reijke TM, Van Tienhoven G, Van den Bergh AC, Oddens J, Poortmans PM, Gez E, Kil P, Akdas A, Soete G, Kariakine O, van der Steen-Banasik EM, Musat E, Piérart M, Mauer ME, Collette L; EORTC Radiation Oncology Group and Genito-Urinary Tract Cancer Group. Duration of androgen suppression in the treatment of prostate cancer. N Engl J Med 2009; 360(24): 2516–2527
8. Amaral TM, Macedo D, Fernandes I, Costa L. Castration-resistant prostate cancer: mechanisms, targets, and treatment. Prostate Cancer 2012; 2012: 327253
9. Basch E, Loblaw DA, Oliver TK, Carducci M, Chen RC, Frame JN, Garrels K, Hotte S, Kattan MW, Raghavan D, Saad F, Taplin ME, Walker-Dilks C, Williams J, Winquist E, Bennett CL, Wootton T, Rumble RB, Dusetzina SB, Virgo KS. Systemic therapy in men with metastatic castration-resistant prostate cancer: American Society of Clinical Oncology and Cancer Care Ontario clinical practice guideline. J Clin Oncol 2014; 32(30): 3436–3448
10. Zhang T, Zhu J, George DJ, Armstrong AJ. Enzalutamide versus abiraterone acetate for the treatment of men with metastatic castration-resistant prostate cancer. Expert Opin Pharmacother 2015; 16(4): 473–485
11. Robinson D, Van Allen EM, Wu YM, Schultz N, Lonigro RJ, Mosquera JM, Montgomery B, Taplin ME, Pritchard CC, Attard G, Beltran H, Abida W, Bradley RK, Vinson J, Cao X, Vats P, Kunju LP, Hussain M, Feng FY, Tomlins SA, Cooney KA, Smith DC, Brennan C, Siddiqui J, Mehra R, Chen Y, Rathkopf DE, Morris MJ, Solomon SB, Durack JC, Reuter VE, Gopalan A, Gao J, Loda M, Lis RT, Bowden M, Balk SP, Gaviola G, Sougnez C, Gupta M, Yu EY, Mostaghel EA, Cheng HH, Mulcahy H, True LD, Plymate SR, Dvinge H, Ferraldeschi R, Flohr P, Miranda S, Zafeiriou Z, Tunariu N, Mateo J, Perez-Lopez R, Demichelis F, Robinson BD, Schiffman M, Nanus DM, Tagawa ST, Sigaras A, Eng KW, Elemento O, Sboner A, Heath EI, Scher HI, Pienta KJ, Kantoff P, de Bono JS, Rubin MA, Nelson PS, Garraway LA, Sawyers CL, Chinnaiyan AM. Integrative clinical genomics of advanced prostate cancer. Cell 2015; 161(5): 1215–1228
12. Cancer Genome Atlas Research Network. The molecular taxonomy of primary prostate cancer. Cell 2015; 163: 1011–1025
13. Liu XL, Wazer DE, Watanabe K, Band V. Identification of a novel serine protease-like gene, the expression of which is down-regulated during breast cancer progression. Cancer Res 1996; 56(14): 3371–3379
14. Hu J, Lei H, Fei X, Liang S, Xu H, Qin D, Wang Y, Wu Y, Li B. NES1/KLK10 gene represses proliferation, enhances apoptosis and down-regulates glucose metabolism of PC3 prostate cancer cells. Sci Rep 2015; 5(1): 17426
15. Czabotar PE, Lessene G, Strasser A, Adams JM. Control of apoptosis by the BCL-2 protein family: implications for physiology and therapy. Nat Rev Mol Cell Biol 2014; 15(1): 49–63
16. Zhang D, Cui Y, Niu L, Xu X, Tian K, Young CY, Lou H, Yuan H. Regulation of SOD2 and β-arrestin1 by interleukin-6 contributes to the increase of IGF-1R expression in docetaxel resistant prostate cancer cells. Eur J Cell Biol 2014; 93(7): 289–298
17. Rajecki M, Sarparanta M, Hakkarainen T, Tenhunen M, Diaconu I, Kuhmonen V, Kairemo K, Kanerva A, Airaksinen AJ, Hemminki A. SPECT/CT imaging of hNIS-expression after intravenous delivery of an oncolytic adenovirus and ^{131}I. PLoS One 2012; 7(3): e32871
18. Barton KN, Stricker H, Elshaikh MA, Pegg J, Cheng J, Zhang Y, Karvelis KC, Lu M, Movsas B, Freytag SO. Feasibility of

adenovirus-mediated hNIS gene transfer and ^{131}I radioiodine therapy as a definitive treatment for localized prostate cancer. Mol Ther 2011; 19(7): 1353–1359

19. Chen X, Wong JY, Wong P, Radany EH. Low-dose valproic acid enhances radiosensitivity of prostate cancer through acetylated p53-dependent modulation of mitochondrial membrane potential and apoptosis. Mol Cancer Res 2011; 9(4): 448–461
20. Ezekwudo D, Shashidharamurthy R, Devineni D, Bozeman E, Palaniappan R, Selvaraj P. Inhibition of expression of anti-apoptotic protein Bcl-2 and induction of cell death in radioresistant human prostate adenocarcinoma cell line (PC-3) by methyl jasmonate. Cancer Lett 2008; 270(2): 277–285
21. Goyal J, Smith KM, Cowan JM, Wazer DE, Lee SW, Band V. The role for NES1 serine protease as a novel tumor suppressor. Cancer Res 1998; 58(21): 4782–4786
22. Li B, Goyal J, Dhar S, Dimri G, Evron E, Sukumar S, Wazer DE, Band V. CpG methylation as a basis for breast tumor-specific loss of NES1/kallikrein 10 expression. Cancer Res 2001; 61(21): 8014–8021
23. Ahmed KA, Davis BJ, Wilson TM, Wiseman GA, Federspiel MJ, Morris JC. Progress in gene therapy for prostate cancer. Front Oncol 2012; 2: 172
24. Spitzweg C, Dietz AB, O'Connor MK, Bergert ER, Tindall DJ, Young CY, Morris JC. *In vivo* sodium iodide symporter gene therapy of prostate cancer. Gene Ther 2001; 8(20): 1524–1531
25. Trujillo MA, Oneal MJ, McDonough S, Qin R, Morris JC. A steep radioiodine dose response scalable to humans in sodium-iodide symporter (NIS)-mediated radiovirotherapy for prostate cancer. Cancer Gene Ther 2012; 19(12): 839–844
26. Zhao LM, Pang AX. Iodine-131 treatment of thyroid cancer cells leads to suppression of cell proliferation followed by induction of cell apoptosis and cell cycle arrest by regulation of B-cell translocation gene 2-mediated JNK/NF-κB pathways. Braz J Med Biol Res 2017; 50(1): e5933